

Investigation of the adsorption characteristics of Cr(VI) onto fly ash, pine nut shells, and modified bentonite

Gang Li^a, Jinli Zhang^{b,*}, Jia Liu^c, Shufeng Chen^a, Huanhuan Li^a

^a*Shaanxi Key Laboratory of Safety and Durability of Concrete Structures, Xijing University, Xi'an, Shaanxi 710123, China, Tel. +86-15991735077; email: T_bag945@126.com (G. Li), Tel. +86-17671777027; email: csf1127@qq.com (S.F. Chen), Tel. +86-15109290717; email: 1020232013@qq.com (H.H. Li)*

^b*State Key Laboratory of Coastal and Offshore Engineering, Dalian University of Technology, Dalian, Liaoning 116024, China, Tel. +86-13940949667; email: jlzhang@dut.edu.cn (J.L. Zhang)*

^c*School of Geological Engineering and Geomatics, Chang'an University, Xi'an, Shaanxi 710054, China, Tel. +86-15929935077; email: 15929935077@163.com (J. Liu)*

Received 21 January 2019; Accepted 27 March 2020

ABSTRACT

Industrial waste or natural materials used as adsorbents for wastewater treatment have the advantage of cost-effective, simple operation, and high efficiency. In this work, batch tests were performed to investigate the adsorption characteristics of Cr(VI) onto fly ash, pine nut shells, and acid-modified bentonite and explore the influence of the solid-to-liquid ratio, pH, ionic strength, and reaction time on adsorption. The results show that the removal rate of the three adsorbents increases with increasing solid-to-liquid ratio, while the unit adsorption capacity decreases. The unit adsorption capacity is maximized when pH = 1–3 and decreases with increasing Cl⁻ concentration. The adsorption of fly ash, pine nut shells, and acid-modified bentonite is a rapid reaction process, of which reaches equilibrium at 180, 120, and 90 min, respectively. The maximum adsorption capacities of fly ash, pine nut shells, and acid-modified bentonite is 0.57, 6.06, and 10.55 mg/g, respectively. The adsorption of Cr(VI) onto fly ash is an exothermic reaction, and the adsorption onto either pine nut shells or acid-modified bentonite is an endothermic reaction. The adsorption of Cr(VI) onto fly ash can be described using the Langmuir, Freundlich, and Redlich–Peterson models, and the pine nut shells can be described by the Langmuir and Redlich–Peterson models, whereas the acid-modified bentonite can be described by the Langmuir, Temkin, and Redlich–Peterson models. The pseudo-second-order kinetic model can accurately describe the kinetic processes of Cr(VI) adsorption onto these adsorbents.

Keywords: Fly ash; Pine nut shell; Bentonite; Cr(VI); Adsorption

1. Introduction

Industrial wastewater contains multiple components, which require a high-cost, complex treatment process. To reduce production costs, some enterprises dispose of industrial wastewater into the municipal wastewater network without any treatment or even underground through

a deep well. Industrial wastewater is different from municipal wastewater, as the former contains various kinds of heavy metal ions and needs special treatment methods. Chromium pollution comes mainly from electroplating, mining, steel manufacturing, leather, and electronic instruments. Most of the chromium exists as Cr(VI) (such as CrO₃, chromate, and dichromate) and Cr(III) (such as chromium oxide and

* Corresponding author.

chromium sulfate). Due to the water solubility and diffusion properties of Cr(VI), in addition to its carcinogenic and mutagenic effects, its toxicity is much higher than that of Cr(III). Frequent contact with a large amount of Cr(VI) may cause an ulcerous discomfort at the contact point. Inhalation of an excessive amount of Cr(VI) may cause liver and kidney failure, cancer, nausea, gastrointestinal irritation, and even death [1]. Generally, heavy metals in industrial wastewater are treated using chemical precipitation [2,3], ion exchange [4,5], membrane treatment [6,7], and biosorption [8–10]. Ion exchange and physical adsorption methods are effective in treating lead [11,12], chromium [13,14], and nickel [15].

Compared to other treatment methods, adsorption methods have the advantage of cost-effective, simple operation, wide pH application range, and high adsorption to heavy metals. Sharma et al. [16–20] investigated the adsorption characteristics and ion exchange of nanocomposite. They found nanocomposite hydrogels show excellent adsorption selectivity for heavy metal ions, and therefore can be used as good bio-adsorbent materials for environmental detoxification. Naushad et al. [21–23] pointed out sodium dodecyl sulfate acrylamide Zr(IV) selenite (SDS-AZS), starch-based nanocomposite (starch/SnO₂) and quaternary amino anion exchanger (Pc-QAE) were successfully used for the adsorbent to the removal of Pb²⁺, Hg²⁺, and phosphate anions, respectively. Pathania et al. [24] studied the ion exchange capacity, and thermal stability of pectin cerium(IV) iodate (PcCeI) and cerium(IV) iodate (CeI) cation ion exchange materials. The results indicated that the selectivity of pectin-cerium(IV) iodate hybrid ion exchange for As³⁺ and Zn²⁺. Al-Othman et al. [25] investigated the adsorption kinetics, equilibrium, and thermodynamics studies on the removal of Cr(VI) by activated carbon. The results showed that the Langmuir model fitted better than the Freundlich model, and the adsorption capacity increased with temperature. Kumar et al. [26] conducted the synthesis of reduced graphene oxide (RGO), polymeric g-C₃N₄, and coal-char (RPC) nano-photocatalysts for efficient solar-powered degradation of noxious emerging pollutants, and they found RPC shows good adsorption activity owing to the high surface area. Huang et al. [27] investigated the adsorption behaviors of fly ash onto quinoline in the aqueous solution, the results indicated that the adsorbed amount increased with the increasing of initial concentration and contact time. Zhou et al. [28] studied the phosphorus adsorption onto coal fly and bottom ash pellet, they found the bottom ash pellet was more suitable adsorbent than fly ash pellet due to the better phosphorus adsorption capacity. Ye et al. [29] investigate the fluoride adsorption onto fly ash modified by lime mud. The results indicated that optimization of the adsorption conditions ensured the realization of the practical needs for fluoride contaminated water. Alouani et al. [30] compared the removal of methylene blue (MB) by fly ash and activated fly ash, they found the maximum monolayer adsorption capacity of fly ash and activated fly ash were 2.88 and 37.08 mg/g, indicating that the activated fly ash is an efficient and low-cost adsorbent for decontamination of dye-containing water. Naushad et al. [31] investigated the isotherms, kinetics, and thermodynamics characteristics of modified pine nut shells onto methylene blue (MB).

The results revealed that maximum MB adsorption reached 39.73 mg/g at pH_i = 5.9, which demonstrated that pine nut shell was a probable cost-effective adsorbent for the removal of MB. Qureshi et al. [32] found the pine nut shell could efficiently remove the toxic phthalates in the aqueous system, as well as in the real water samples. Esmaili and Eslami [33] investigated the adsorption of Pb(II) and Zn(II) onto natural bentonite. The results revealed that the removal efficiency of Pb(II) and Zn(II) were increased with increasing of the initial pH, adsorbent dose, and contact time, and the adsorption efficiency of Pb(II) was larger than Zn(II). Sahan [34] studied the Pb(II) and Cu(II) adsorption onto bentonite enriched with-SH groups (BSH). They pointed out that the maximum removal rate of Pb(II) and Cu(II) were 95.05% and 91.4%, respectively, which indicated that BSH has great potential applications in the removal of heavy metal. Cheng et al. [35] found the bentonite modified by aluminum cross-linking and tannin double modification has excellent removal performance for ammonia nitrogen in low temperature wastewater. Sadeghalvad et al. [36] investigated the adsorption behaviors of Ni(II) onto bentonite, and the statistical method was used to evaluate the maximum adsorption amount of Ni(II). Souza et al. [37] investigated the kinetics of crystal violet (CV) adsorption on bentonite by pore volume and surface diffusion model, surface diffusion model, and pore volume diffusion model. Mdalose et al. [38] studied the adsorption of phosphate ions from water by bentonite modified with Fe, Co, and Ni salts. The results indicated that metal-modified bentonite have lower crystallinity compared to the native bentonite, and the competition effect of coexisting anions were not significant for Fe and Ni modified bentonite.

To date, relatively few studies have been conducted to examine the adsorption behaviors of Cr(VI) onto natural or waste materials. In this work, we used fly ash, pine nut shells, and acid-modified bentonite as adsorbents and investigated their adsorption characteristics for Cr(VI) using batch experiments. The influence of the solid-to-liquid ratio, pH, initial Cr(VI) concentration, temperature, reaction time, and ionic strength on the adsorption of Cr(VI) was analyzed. The adsorption kinetic characteristics, isothermal adsorption characteristics, and thermodynamic characteristics are discussed. The research results provide a reference for removal of Cr(VI) from wastewater.

2. Materials and methods

2.1. Experimental materials and instruments

The fly ash, pine nut shells, and bentonite used in this experiment were natural materials, the fly ash was obtained from Dalian Taishan Power Plant of Liaoning Province, China, the pine nut shells were from red pine nuts from Northeast China (the kernels were removed), and the bentonite was from the Heishan area of Liaoning Province, China. As shown in Table 1, fly ash was mainly composed of SiO₂, CaO, Al₂O₃, and Fe₂O₃. Fly ash particles were porous honeycomb structure with large specific surface area and high adsorption activity. The particle size ranges from 0.5 to 300 μm, and the porosity was as high as 50%–80%. Pine nut shell was widely distributed in China and annual output

Table 1
Chemical composition of fly ash, pine nut shell, and bentonite

Fly ash		Pine nut shell		Bentonite	
Component	Mass percent (%)	Component	Mass percent (%)	Component	Mass percent (%)
SiO ₂	50.4	C	98.9	SiO ₂	70.7
CaO	25.0	K ₂ O	0.339	Al ₂ O ₃	14.3
Al ₂ O ₃	9.08	SiO ₂	0.148	K ₂ O	4.38
Fe ₂ O ₃	8.39	Na ₂ O	0.141	CaO	2.99
SO ₃	2.77	SO ₃	0.116	Fe ₂ O ₃	2.94
MgO	1.04	Al ₂ O ₃	0.106	MgO	2.00
K ₂ O	0.986	P ₂ O ₅	0.0826	Na ₂ O	1.91
P ₂ O ₅	0.700	Fe ₂ O ₃	0.0566	TiO ₂	0.241
Na ₂ O	0.658	CaO	0.0537	BaO	0.197
TiO ₂	0.507	Cl	0.0206		
SrO	0.215				
BaO	0.191				

was huge, mainly composed of C, K₂O, SiO₂, and Na₂O. Meanwhile, it mainly consists of lignin, cellulose, and hemicellulose. Bentonite was mainly composed of SiO₂, Al₂O₃, K₂O, and CaO, and the main mineral component was montmorillonite. The physical and chemical structure of montmorillonite leads to its excellent ion exchange, expansibility, and dispersibility, which was widely used in environmental remediation and wastewater treatment.

The fly ash, pine nut shells, and bentonite were crushed using a crushing machine and passed through a 60-mesh geogrid. They were then placed in a DHG-9011A type oven (Shanghai Jinghong laboratory Instrument Co., Ltd., China) at 60°C for 24 h and passed through the 60 mesh geogrid again. The powders were then stored in desiccators for future usage. The main chemical compositions of the three samples were analyzed by SRS3400 type total-reflection X-ray fluorescence spectrometer (Bruker, Germany), and the results are listed in Table 1. Moreover, concentrated nitric acid was used to modify the bentonite. The concentrated nitric acid was injected into the distilled water slowly by passing through a glass rod while the solution was slowly stirred. The concentrated nitric acid was diluted to 1 mol/L and allowed to stand for 12 h before future usage. A bentonite sample of 30 g was weighed and poured into 500 mL of diluted nitric acid solution. The solution was slowly stirred to turbid liquid and allowed to stand for 24 h after bentonite particles precipitated to the bottom of the beaker. The acid in the beaker was transferred into the water bottle using a pipette, and the remaining saturated bentonite sample was filtered using filter paper and dried in a 60°C oven for 48 h. The sample was then crushed and passed through the 60 mesh geogrid to obtain the acid-modified bentonite sample.

Potassium dichromate (K₂Cr₂O₇, guaranteed reagent grade) (Tianjin Chemical Reagent Co., Ltd., China) was placed in an oven at 120°C and dried for 2 h. Potassium dichromate was weighed (0.2829 g) and dissolved in a volumetric flask (Tianjin Tianbo Glass Instrument Co., Ltd., China) with distilled water by shaking. After all potassium dichromate was dissolved, distilled water was added until the total volume of the solution reached 1,000 mL to obtain

a Cr(VI) stock liquor of 100 mg/L concentration. The solution was allowed to stand for 12 h before usage. All Cr(VI) solution used in this experiment was diluted from the aforementioned stock liquor.

2.2. Experimental methods

2.2.1. Adsorption tests

Adsorption tests were performed using a batch method. First, the stock liquor was diluted to the desired concentration. 50 mL of the diluted solution was introduced into a numbered Erlenmeyer flask (Tianjin Tianbo Glass Instrument Co., Ltd., China). Each solid adsorbent was weighed to make samples with the desired solid-to-liquid ratio and added to an Erlenmeyer flask. The flasks were then placed in a SHA-C type thermostatic oscillator (Changzhou Guohua Electric Appliance Co., Ltd., China) with temperature adjusted according to the predesigned experimental conditions. The rotating rate of the oscillator was set at 120 rpm, and samples were oscillated for 12 h. After the reaction, the solutions were removed from the Erlenmeyer flasks, transferred into a CT15RT type centrifuge machine (Shanghai Tianmei Biochemical Engineering Equipment Co., Ltd., China), and centrifuged at 3,000–5,000 rpm for 20–30 min. The supernatant solution was isolated, and its Cr(VI) concentration and the equilibrium pH (pH_e) were measured using an AA6000 type atomic absorption spectrophotometer (Shanghai Tianmei Biochemical Engineering Equipment Co., Ltd., China) and a Starter2C type pH meter (Shanghai Ohaus Instruments Co., Ltd., China).

An isothermal adsorption experiment was also carried out using a batch method. Batch tests were performed at different temperatures through adjusting the temperature of the oscillator. The influence of the temperature on the adsorption characteristics was analyzed by comparing the test data.

2.2.2. Kinetic test

The kinetic test used a sampling interval of 1 h, when samples were observed for equilibrium to predict the test

duration. The influence of the reaction time on the adsorption characteristics was observed by adjusting the sampling interval.

2.2.3. Desorption test

During the desorption test, the adsorbent was filtered by the filter paper three times after the isothermal adsorption reaction and dried at 60°C for 48 h before passing through the 60-mesh geogrid. Distilled water was added dropwise to prepare a solution with the desired solid-to-liquid ratio. The Cr(VI) content in the solution was measured using a batch method.

The adsorption capacity q_e (mg/g), removal rate R (%), and solid-to-liquid ratio r (g/L) at equilibrium were calculated using the equations below:

$$q_e = \frac{(C_0 - C_e)}{m} \times V \quad (1)$$

$$R(\%) = \frac{(C_0 - C_e)}{C_0} \times 100 \quad (2)$$

$$r = \frac{m}{V} \quad (3)$$

where C_0 and C_e are the initial and equilibrium concentrations of heavy metal ions in the solution (mg/L), respectively. V is the volume of the solution (L), m is the mass of the clay or bentonite (g).

2.3. Theoretical model

2.3.1. Isothermal adsorption model

The equation describing the adsorption isothermal curve is called the isothermal adsorption model. In this paper, Langmuir model, Freundlich model, Temkin model, and Redlich–Peterson model were used to fit the isothermal adsorption test data, and the adsorption characteristics of the Cr(VI) onto three adsorbents were analyzed.

(a) Langmuir model [39]

$$\frac{C_e}{q_e} = \frac{1}{bQ} + \frac{C_e}{Q} \quad (4)$$

where q_e is the adsorption capacity (mg/g) of heavy metal ions at adsorption equilibrium, Q is the single-layer maximum adsorption capacity (mg/g) of the adsorbent, and b is the Langmuir model constant (L/mg).

$$R_L = \frac{1}{1 + bC_0} \quad (5)$$

The value of the dimensionless separation factor R_L can indicate whether the adsorption reaction is favorable [40]. When $0 < R_L < 1$, the reaction is favorable for adsorption; when $R_L > 1$, it is unfavorable for adsorption. When $R_L = 1$, the adsorption is reversible, when $R_L = 0$, it is irreversible [41].

(b) Freundlich model [42]

$$\log q_e = \log K_F + \frac{1}{n} \log C_e \quad (6)$$

where K_F is the model constant, which is related to the adsorption capacity (mg/g), and n is the model constant that is related to adsorption strength.

(c) Temkin model [43]

$$q_e = \frac{RT}{b_T} \ln K_T + \frac{RT}{b_T} \ln C_e \quad (7)$$

where b_T is the Temkin constant related to the heat of sorption (kJ/mol), K_T is the equilibrium binding constant corresponding to the maximum binding energy (L/g), T is the absolute temperature (K), and R is the gas constant (8.314×10^{-3} kJ/mol/K). The values of K_T and b_T were obtained from the slope and intercept of a straight line plot of q_e vs. $\ln C_e$.

(d) Redlich–Peterson model [44]

$$q_e = \frac{PC_e}{1 + \alpha C_e^\beta} \quad (8)$$

where α (L/mg) and β are the isotherm constants.

2.3.2. Adsorption kinetic model

According to different adsorption mechanisms and assumption conditions, several adsorption kinetic models were developed to study the adsorption process of the adsorbate onto the adsorbent and the rate of adsorption. In this paper, the pseudo-first-order kinetic model and pseudo-second-order kinetic model were used to describe the kinetic adsorption process of the three adsorbents.

(a) Pseudo-first-order kinetic model [45]

$$\ln(q_e - q_t) = \ln q_e - k_1 t \quad (9)$$

where q_t and q_e are the adsorbed amounts at time t , and at equilibrium, respectively, and k_1 is the rate constant for pseudo-first-order adsorption (1/min). The values of rate constants were determined from the slope of the plot $\ln(q_e - q_t)$ vs. t .

(b) Pseudo-second-order kinetic model [46]

$$\frac{dq_t}{dt} = k_2 (q_e - q_t)^2 \quad (10)$$

Its integral is:

$$\frac{t}{q_t} = \frac{1}{k_2 q_e^2} + \frac{1}{q_e} t \quad (11)$$

where k_2 is the adsorption rate constant (g/mg/min), q_t and q_e are adsorption capacities at time t and equilibrium (mg/g), respectively, and h is the initial adsorption rate (g/mg/min).

When t approaches 0, h can be expressed as:

$$h = k_2 q_e^2 \tag{12}$$

2.3.3. Adsorption thermodynamic model [47]

The adsorption thermodynamic equation can be expressed as:

$$K_D = \frac{q_e}{C_e} \tag{13}$$

$$\ln K_D = \frac{\Delta S}{R} - \frac{\Delta H}{RT} \tag{14}$$

$$\Delta G = \Delta H - T\Delta S \tag{15}$$

where C_e is the metal ion concentration in the supernatant at the equilibrium, q_e is the adsorption capacity at the equilibrium, K_D is the distribution coefficient at the solid-liquid interface (mL/g), R is the molar gas constant (8.314 J/mol/K), T is the thermodynamic temperature (K), ΔH is the enthalpy change (kJ/mol), ΔS is the entropy change (J/mol/K), and ΔG is the Gibbs free energy (kJ/mol).

3. Results and discussion

3.1. Influence of the solid-to-liquid ratio on Cr(VI) adsorption

Tests were carried out at 20°C on solutions with different initial Cr(VI) concentrations of 10, 25, and 50 mg/L.

The pH value ($\text{pH}_0 = 5.5$) was not adjusted during the test. The influence of the solid-to-liquid ratio r on the adsorption capacity q_e and removal rate R of Cr(VI) by the fly ash, pine nut shells, and bentonite were analyzed by adjusting the solid-to-liquid ratio. For fly ash, the solid-to-liquid ratio were 20, 50, 100, 200, 400, and 600 g/L, whereas the solid-to-liquid ratio were 1, 2, 5, 10, 20, and 50 g/L for pine nut shells and bentonite, the results are shown in Fig. 1. The removal rate of Cr(VI) by fly ash, pine nut shells, and bentonite increases, and adsorption capacity decreases with increasing solid-to-liquid ratio. The main reason is that when the amount of adsorbent increases, its surface area and the number of available adsorption sites also increase [48], which results in an increase of the removal rate. However, the decrease of the adsorption capacity is due to the incomplete mixing of adsorbent particles and the solution, where only part of the adsorption sites is exposed. For solutions with different initial concentrations of Cr(VI), a lower solid-to-liquid ratio results in higher adsorption capacity. However, due to the limited mass of adsorbent, the removal rate to Cr(VI) in the solution is low. With increasing solid-to-liquid ratio, the adsorption capacity decreases, but the removal rate increases. Therefore, a high solid-to-liquid ratio is preferred when using fly ash to adsorb Cr(VI), and a low solid-to-liquid ratio is preferred when using pine nut shell and bentonite.

As shown in Fig. 1c, when the solid-to-liquid ratio reaches 50 g/L, the highest removal rate of bentonite is only 60%. Clearly, the capability of bentonite to adsorb Cr(VI) is low. Therefore, concentrated nitric acid was used to modify the bentonite. Tests were carried out at the same condition as the bentonite, the results as shown in Fig. 1d. When

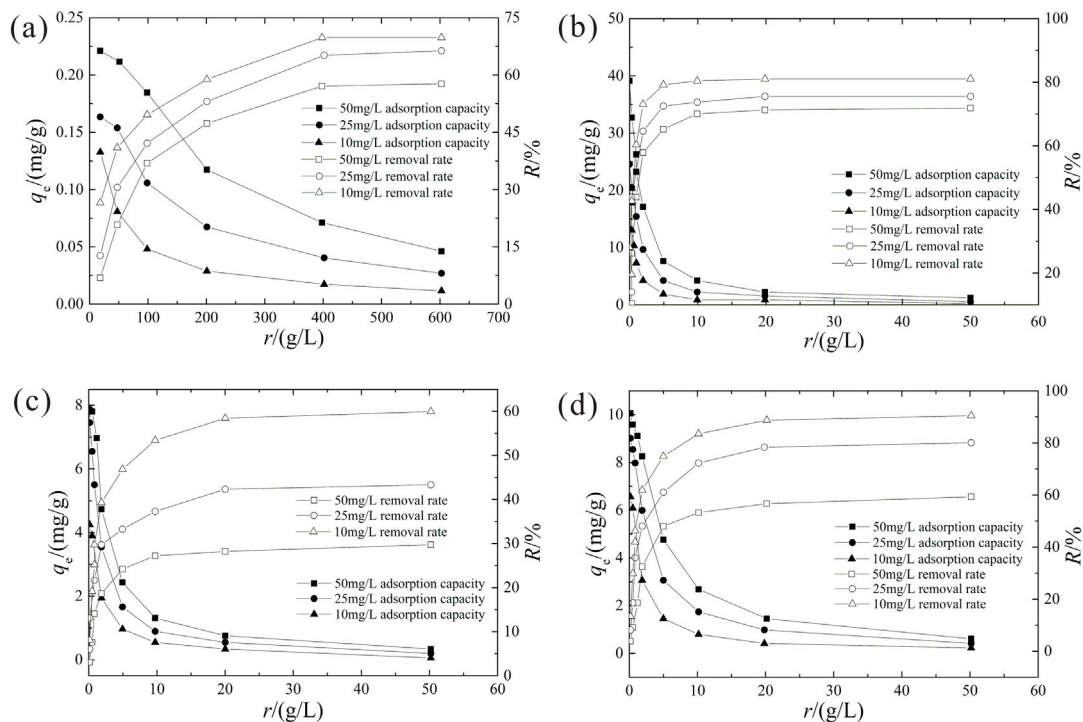


Fig. 1. Effect of solid-to-liquid ratio on Cr(VI) adsorption (a) fly ash, (b) pine nut shell, (c) bentonite, and (d) H⁺-bentonite.

the solid-to-liquid ratio reaches 20 g/L, the removal rate of acid-modified bentonite nearly reaches 90% of the maximum removal rate. Any further increase in the solid-to-liquid ratio has a less significant effect on the removal rate. With a gradual increase in the solid-to-liquid ratio, the adsorption capacity decreases, and the removal rate is enhanced. A comparison between Figs. 1c and d show that the effect of acid-modified bentonite is significantly better than the original bentonite sample in the removal of Cr(VI).

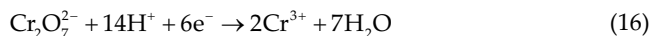
3.2. Influence of the pH on Cr(VI) adsorption

To analyze the influence of the pH value on the adsorption characteristics of the fly ash, pine nut shells, and modified bentonite, tests were performed at a temperature of 20°C. For fly ash, a solid-to-liquid ratio was 100 g/L, and an initial concentration was 50 mg/L. For pine nut shells, the solid-to-liquid ratio and initial concentration was 10 g/L and 50 mg/L, respectively. Whereas, tests were performed at a solid-to-liquid ratio was 2 g/L, an initial concentration was 10 mg/L for acid-modified bentonite. HNO₃ and NaOH were used as buffers to adjust the initial pH (pH₀) of the solution, and the influence of the pH on the removal rate was analyzed. Furthermore, the pH value (pH_e) when the adsorption reaction reached equilibrium was also measured; the results are shown in Fig. 2.

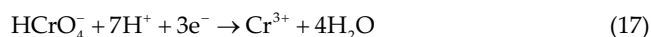
The capability of adsorbents to adsorb Cr(VI) and the removal rate of Cr(VI) decreases significantly when pH₀ increases, which indicates that the acidic environment is favorable to the adsorption of Cr(VI). For fly ash, the removal rate changes slowly when pH₀ reaches 5.5, whereas when pH₀ reaches 7.0 and 8.5 for pine nut shell and acid-modified bentonite, respectively. For a low pH₀ value, Cr(VI) in the

solution exists in the forms of HCrO₄⁻ and Cr₂O₄²⁻ [49], and that low pH is favorable for the conversion of Cr⁶⁺ to Cr³⁺.

In strong acidic environments:



In a neutral environment:



In strong acidic environments, a large amount of H⁺ exists in the solution, which can neutralize the negative charges on the surface of the adsorbents. This neutralization reaction is favorable for the diffusion of HCrO₄⁻ and Cr₂O₄²⁻ on the surface of the adsorbents. When the pH increases, due to the limit of the double electric layer on the surface of the adsorbents, the double electric layer on the surface of adsorbents converts from positive to negative, which is unfavorable for the adsorption reaction. Therefore, a higher pH of the solution results in a lower removal rate of Cr(VI).

In addition, metal ions, such as Fe and Al, may dissolve on the surface of the adsorbent particles, thus changing the porous property of the adsorbent and increasing the number of adsorption sites on the surface of the adsorbent [50]. The measurement of potentials on the surface of adsorbents shows that the surface has a strong positive zeta potential in the acidic environment and thus adsorbs negative ions [51], which is consistent with the results presented here. The equilibrium pH (pH_e) was also measured during the test and was found to increase dramatically for pine nut shell and acid-modified bentonite, and changes slowly for fly ash when pH₀ reached 5.5, indicating that oxides such as

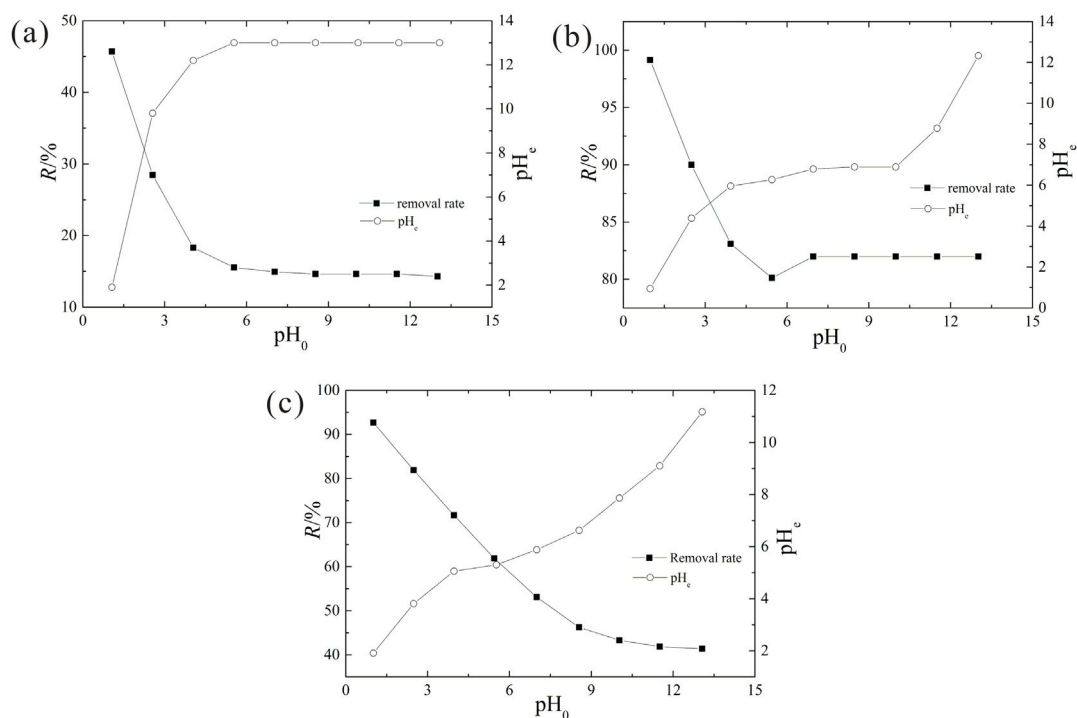


Fig. 2. Effect of pH on Cr(VI) adsorption (a) fly ash, (b) pine nut shell, and (c) H⁺-bentonite.

CaO, Al₂O₃, and MgO react with water and generate a large amount of OH⁻ [52].

3.3. Influence of the ionic strength on Cr(VI) adsorption

To analyze the ionic strength effect on the Cr(VI) adsorption, the experiments were conducted at a reaction temperature of 20°C, the effect of ionic strength on Cr(VI) adsorption onto adsorbents was analyzed through addition of different concentrations of NaCl to adjust the concentration of Cl⁻ in the range of 0–0.5 mol/L. For fly ash, a solid-to-liquid ratio was 100 g/L, and an initial concentration was 50 mg/L. For pine nut shells, the solid-to-liquid ratio and initial concentration was 10 g/L and 50 mg/L, respectively. Whereas, tests were performed at a solid-to-liquid ratio was 2 g/L, an initial concentration was 10 mg/L for acid-modified bentonite. The results shown in Fig. 3, it reveals that the removal rate of fly ash, pine nut shells, and acid-modified bentonite to Cr(VI) decreases with increasing Cl⁻ concentration. When the ionic strength increases from 0.0 to 0.5 mol/L, the removal rate of Cr(VI) decreases 23.41%, 27.87%, and 28.78%, respectively. As the ionic strength increases, the thickness of the diffusion layer decreases due to the increasing electrolyte concentration. The electrical double layer is compressed, the distance between ions and soil particles at collision decreases, and the attractive force between them increases. The increasing extent in the attractive force is lower than the extent of competition between Na⁺ and Cr⁶⁺ for adsorption sites. Therefore, the removal rate of Cr(VI) keeps decreases. In addition, the measured pH (not adjusted during the test) was approximately 5.5, which means that the solution was in an acidic environment,

and Cr(VI) mainly existed in forms of HCrO₄⁻ and Cr₂O₄²⁻. Cl⁻ and Cr(VI) competed for active adsorption sites, resulting in a dramatic decrease of adsorption capability. The experimental results reveal that the adsorption capability of fly ash, pine nut shells, and acid-modified bentonite to Cr(VI) is significantly affected by the anionic strength.

3.4. Adsorption kinetic characteristics of Cr(VI)

The relationship between reaction time and capacity of adsorbents to adsorb Cr(VI) was analyzed at temperatures of 20°C, 30°C, and 40°C; and the pH (pH₀ = 5.5) was not adjusted during the test. For fly ash, a solid-to-liquid ratio was 100 g/L, and an initial concentration was 50 mg/L. For pine nut shells, the solid-to-liquid ratio and initial concentration was 10 g/L and 50 mg/L, respectively. Whereas, tests were performed at a solid-to-liquid ratio was 2 g/L, an initial concentration was 10 mg/L for acid-modified bentonite. The results are shown in Fig. 4.

The adsorption of Cr(VI) includes three continuous kinetic processes: diffusion outside the particles, diffusion in pores, and an adsorption reaction [53]. Fig. 3a shows that the removal of Cr(VI) by fly ash is a rapid reaction process in which the adsorption capacity reaches 75% of the maximum adsorption within the first 30 min of the reaction. The adsorption capacity no longer increases at 180 min, which shows that the adsorption reaction reaches equilibrium. Fig. 3b shows that the adsorption capacity of Cr(VI) onto pine nut shells reaches 80% of the maximum adsorption capacity in the first 20 min of the reaction and the adsorption reaction reaches equilibrium at 120 min. Fig. 3c shows that the adsorption capacity of Cr(VI) onto acid-modified

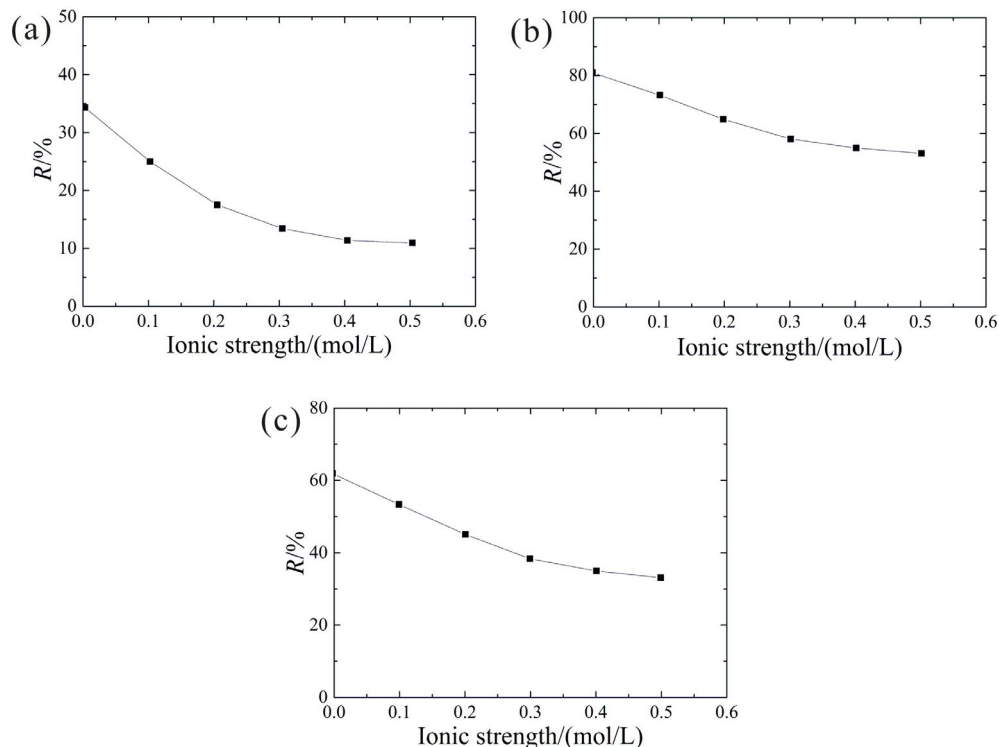


Fig. 3. Effect of ionic strength on Cr(VI) removal rate (a) fly ash, (b) pine nut shell, and (c) H⁺-bentonite.

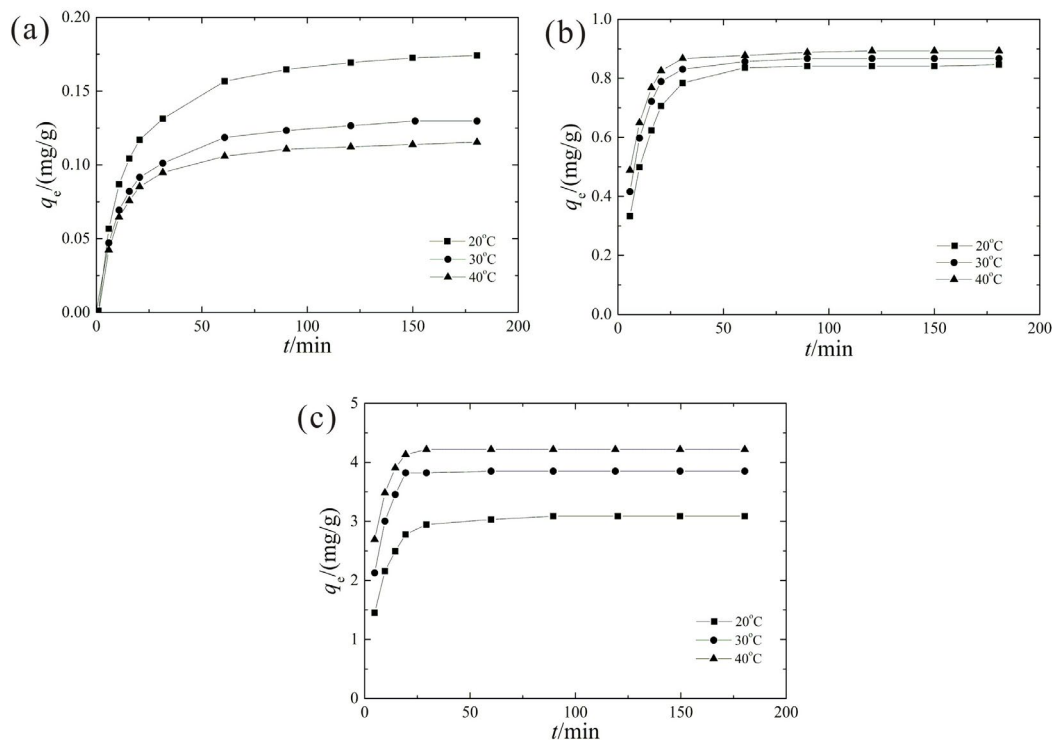


Fig. 4. Effect of reaction time on Cr(VI) adsorption (a) fly ash, (b) pine nut shell, and (c) H⁺-bentonite.

bentonite reaches 90% of the maximum adsorption in the first 20 min of the reaction. The adsorption capacity stabilizes at 90 min. The main reason of this phenomenon is that there are more adsorption sites on the surface of the adsorbent at the beginning of the reaction, which is favorable to the adsorption of Cr(VI) in the solution. With increasing reaction time, the adsorption sites on the surface of the adsorbent gradually decrease, which decreases the reaction rate of Cr(VI) adsorption.

To describe the adsorption kinetic characteristics of Cr(VI) onto adsorbents, a pseudo-first-order kinetic model and a pseudo-second-order kinetic model were used to fit and analyze the test data, the results are shown in Fig. 5 and Table 2. Table 2 shows that a high coefficient of determination was obtained using the pseudo-second-order kinetic model than pseudo-first-order kinetic model to fit the test results. The pseudo-second-order kinetic model assumes that the adsorption process includes two stages of rapid adsorption and slow adsorption. The adsorption reaction process of Cr(VI) is consistent with this assumption. Therefore, the kinetic processes of Cr(VI) adsorption onto the fly ash, pine nut shells, and acid-modified bentonite can be accurately simulated using the pseudo-second-order kinetic equation.

3.5. Isothermal adsorption characteristics of Cr(VI)

The isothermal adsorption characteristics of Cr(VI) onto adsorbents were analyzed at a reaction time of 12 h, and temperatures of 20°C, 30°C, and 40°C. The adsorption tests were performed at an initial concentration was varied from 5 to 50 mg/L. For fly ash, a solid-to-liquid ratio was 100 g/L. For pine nut shells and acid-modified bentonite, the

solid-to-liquid ratio was 10 and 2 g/L, respectively. As shown in Fig. 6a, the adsorption capacity of fly ash to adsorb Cr(VI) increases gradually with increasing Cr(VI) concentration at the same solid-to-liquid ratio and temperature, which shows that the adsorption sites of the fly ash have not reached saturation. When the temperature is controlled at 20°C, 30°C, and 40°C, the adsorption capability of the fly ash decreases with increasing temperature, which indicates that the adsorption reaction of Cr(VI) onto the fly ash is an exothermic reaction and that higher temperatures are unfavorable to adsorption. As shown in Figs. 6b and c, the adsorption capacity of Cr(VI) onto pine nut shells and acid-modified bentonite increases with increasing initial Cr(VI) concentration at the same solid-to-liquid ratio and temperature, which shows that the utilization rate of the adsorption sites of pine nut shells is affected by the initial concentration of Cr(VI), and a higher initial concentration of Cr(VI) corresponds to more adsorption sites. The adsorption capability of pine nut shells and acid-modified bentonite increases slightly with increasing temperature, which reveals that the adsorption reaction of Cr(VI) onto pine nut shells is an endothermic reaction and that higher temperatures favor adsorption.

The Langmuir model, Freundlich model, Temkin model, and Redlich–Peterson model were used to describe the isothermal adsorption process of Cr(VI), the results are shown in Fig. 7, and the corresponding model parameters are shown in Table 3. For fly ash, Langmuir model, Freundlich model, and Redlich–Peterson model can accurately fit the test results (the coefficient of determination R^2 is high). By calculation, all R_L values are less than 1, indicating that the adsorption of Cr(VI) onto fly ash is favored. Table 3 shows that $n > 1$, and the curve is a type I curve (upper convex),

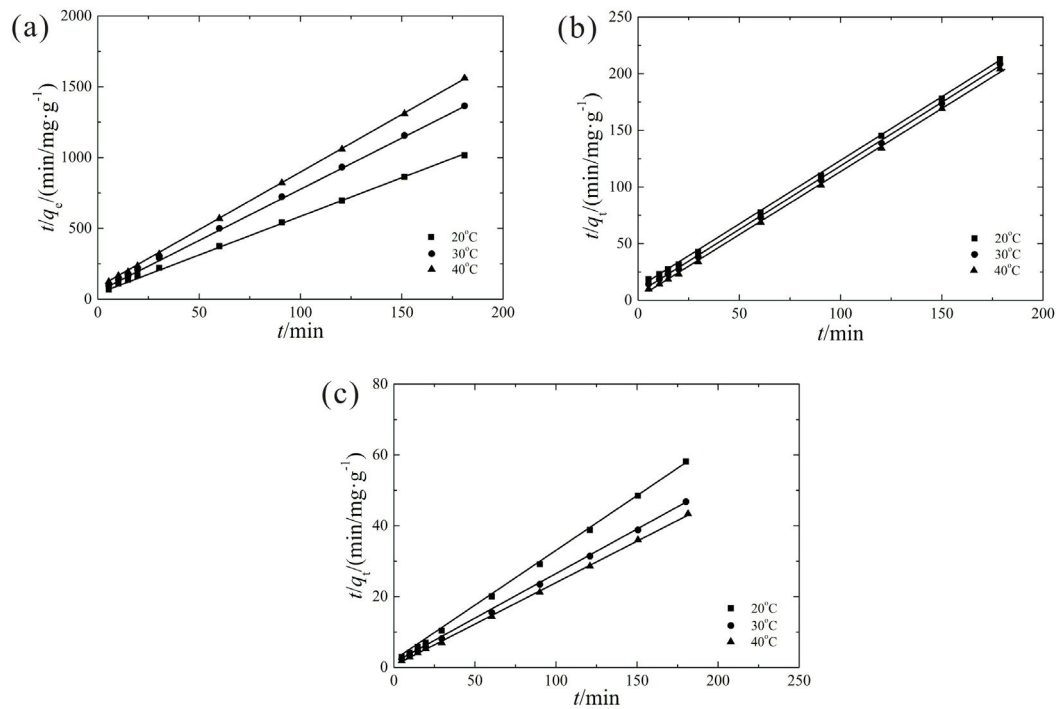


Fig. 5. Fitting the data of Cr(VI) adsorption with the pseudo-second-order kinetic model (a) fly ash, (b) pine nut shell, and (c) H⁺-bentonite.

Table 2
Model parameters of the kinetic models for Cr(VI) adsorption

Adsorbents	T (°C)	Pseudo-first-order kinetic			Pseudo-second-order kinetic		
		q_e (mg/g)	k_1 (1/min)	R^2	q_e (mg/g)	k_2 (1/min)	R^2
Fly ash	20	0.125	0.031	0.9918	0.187	0.453	0.9997
	30	0.085	0.029	0.9834	0.138	0.711	0.9999
	40	0.073	0.034	0.9845	0.121	0.965	0.9997
Pine nut shell	20	0.337	0.059	0.9150	0.877	0.205	0.9991
	30	0.449	0.068	0.9675	0.884	0.327	0.9996
	40	0.798	0.084	0.9996	0.906	0.392	0.9998
H ⁺ -bentonite	20	2.781	0.111	0.9978	3.178	0.082	0.9996
	30	3.989	0.167	0.9416	3.908	0.131	0.9996
	40	4.337	0.194	0.9907	4.259	0.166	0.9998

indicating that an affinity that boosts the adsorption exists between the surface of the adsorbent and adsorbate. For pine nut shells, Langmuir model, and Redlich–Peterson model fitting results are consistent with the test results, and the coefficient of determination R^2 is high. Therefore, the Langmuir model and Redlich–Peterson model were used to simulate the isothermal adsorption process of Cr(VI) onto pine nut shells. All calculated R_L values are less than 1, which indicates that the adsorption of Cr(VI) onto pine nut shells is favored. For acid-modified bentonite, Langmuir model, Temkin model, and Redlich–Peterson model are consistent with the test results and that the coefficient of determination R^2 is high, indicating that the models can accurately simulate the isothermal adsorption

process of Cr(VI). All calculated R_L values are less than 1, which indicates that the acid-modified bentonite is favorable for adsorption of Cr(VI). However, the fitting results of Freundlich model are not well and the coefficient of determination R^2 is low, indicating that Freundlich model cannot simulate the isothermal adsorption process of Cr(VI) onto acid-modified bentonite.

3.6. Thermodynamic adsorption characteristics of Cr(VI)

To analyze the adsorption thermodynamic properties of Cr(VI) onto fly ash, pine nut shells, and acid-modified bentonite, the adsorption thermodynamic model was used for calculation. The adsorption activation energy and

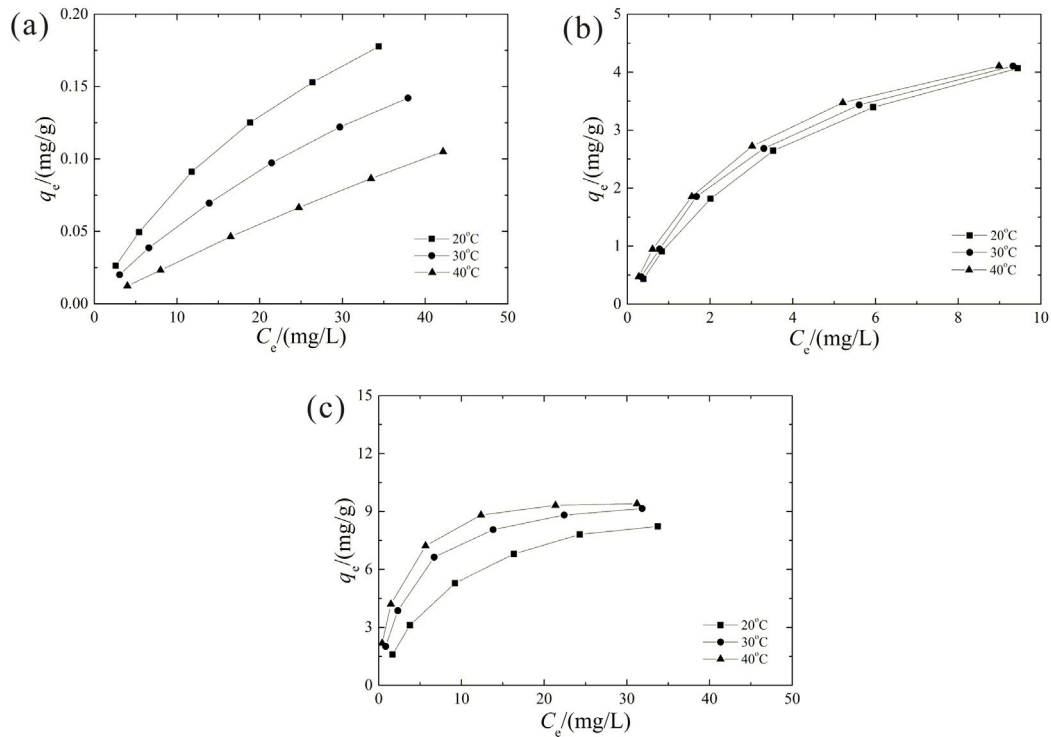


Fig. 6. Isothermal adsorption curves of Cr(VI) under different temperatures (a) fly ash, (b) pine nut shell, and (c) H⁺-bentonite.

Table 3
Model parameters of isothermal adsorption models for Cr(VI) adsorption

Models	Parameters	Fly ash			Pine nut shell			H ⁺ -bentonite		
		20°C	30°C	40°C	20°C	30°C	40°C	20°C	30°C	40°C
Langmuir	Q (mg/g)	0.335	0.344	0.565	6.060	5.570	5.430	10.554	10.274	10.440
	b (L/g)	0.035	0.020	0.006	0.215	0.289	0.338	9.091	3.810	2.137
	R_L	0.367	0.502	0.778	0.085	0.065	0.056	0.011	0.026	0.045
	R^2	0.9994	0.9999	0.9996	0.9997	0.9993	0.9988	0.9993	0.9999	0.9997
Freundlich	K_F (mg/g)	0.014	0.008	0.004	1.003	1.130	1.219	1.412	2.319	3.233
	N	1.346	1.239	1.082	1.460	1.558	1.606	1.856	2.267	2.821
	R^2	0.9929	0.9964	0.9994	0.9789	0.9742	0.9754	0.9649	0.9515	0.9500
Temkin	b_T (J/mol)	41.535	52.074	67.327	2.095	2.244	2.425	1.057	1.228	1.452
	K_T	0.493	0.392	0.266	2.972	3.611	4.507	1.118	3.219	8.267
	R^2	0.9848	0.9771	0.9663	0.9896	0.9810	0.9920	0.9980	0.9956	0.9916
Redlich–Peterson	P (L/g)	0.011	0.007	0.003	1.328	1.563	1.883	1.248	2.831	5.878
	α (L/g)	0.057	0.035	0.010	0.236	0.276	0.371	0.144	0.283	0.669
	B	0.863	0.865	0.866	0.968	0.997	0.970	0.946	0.994	0.959
	R^2	0.9999	0.9998	0.9999	0.9996	0.9992	0.9999	0.9995	0.9995	0.9992

thermodynamic parameters are listed in Table 4. For fly ash, the enthalpy change (ΔH) of the dry reaction is less than 0, indicating that the adsorption reaction process of Cr(VI) onto fly ash is exothermic. The negative change in Gibbs free energy (ΔG) reveals that the adsorption reaction is spontaneous [54]. For pine nut shells, the enthalpy change (ΔH) is greater than 0, indicating the adsorption reaction process of Cr(VI) onto pine nut shells is an

endothermic reaction (i.e., higher temperatures promote adsorption). The positive change in the Gibbs free energy (ΔG) reveals that the adsorption reaction is not spontaneous. For acid-modified bentonite, the activation energy E_a is negative, indicating that the adsorption mechanism is mainly one of ionic exchange. The enthalpy change (ΔH) is positive, indicating that the adsorption reaction process of Cr(VI) is an endothermic reaction, that is, one promoted

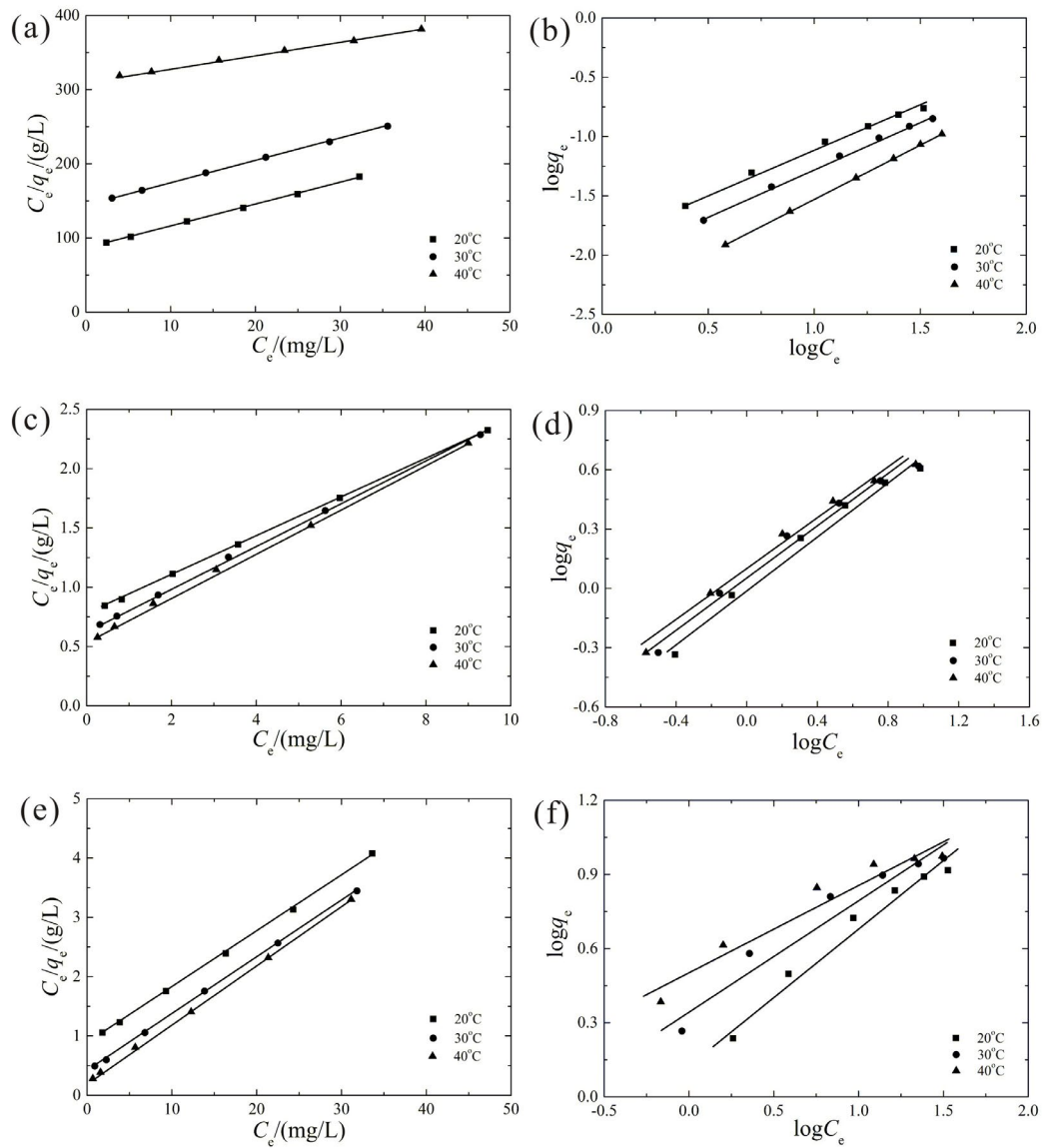


Fig. 7. Fitting curves of the isotherm model for Cr(VI) adsorption under different temperature (a) Langmuir model with fly ash, (b) Freundlich model with fly ash, (c) Langmuir model with pine nut shell, (d) Freundlich model with pine nut shell, (e) Langmuir model with H⁺-bentonite, and (f) Freundlich model with H⁺-bentonite.

Table 4
Thermodynamic parameters for Cr(VI) adsorption

Adsorbents	E_a (kJ/mol)	ΔH (J/mol)	ΔS (J/mol/K)	ΔG (J/mol)		
				293 K	303 K	313 K
Fly ash	28.997	-248.913	-0.074	-30.736	-23.294	-15.851
Pine nut shell	60.053	2,214.385	0.517	2,062.946	2,057.780	2,052.614
H ⁺ -bentonite	-3.455	5,543.098	23.628	-1,383.45	-1,619.73	-1,856.01

Table 5
Comparison of maximum adsorption capacities of Cr(VI) between different adsorbents

Adsorbent	pH	T (°C)	r (g/L)	C_0 (mg/L)	q_m (mg/g)	References
Natural Akadama clay	2	25	5	5–50	4.29	[55]
Tobacco residues	8	20	4	6	0.55	[56]
<i>Aegle marmelos</i> fruit shell	2	40	3	2–10	4.27	[57]
Sugarcane bagasse	2	25	20	50	0.63	[58]
Maize corn cob	2	25	20	50	0.28	[58]
Jatropha oil cake	2	25	20	50	0.82	[58]
Volcanic rocks	2	22	100	0.5–10	0.05	[59]
Riverbed sand	2.5	25	20	1.05–7.84	0.15	[60]
Turkish montmorillonite clay	1	20	10	250	3.61	[61]
Orange peels powder	7	–	25	5–25	4.69	[62]
Fly ash	5.5	40°C	100	5–50	0.57	This study
Pine nut shells	5.5	20°C	10	5–50	6.06	This study
Acid-modified bentonite	5.5	20°C	2	5–50	10.55	This study

at higher temperatures. The negative change of Gibbs free energy (ΔG°) reveals that the adsorption reaction is spontaneous.

3.7. Adsorption stability

The samples of fly ash, pine nut shell, and acid-modified bentonite after adsorption were filtered using filter paper three times after the adsorption reaction and dried at 60°C for 48 h. Distilled water was added to prepare samples with a solid-to-liquid ratio was 5 g/L for batch tests. No Cr(VI) was detected in the solution, indicating that fly ash, pine nut shell, and acid-modified bentonite with adsorbed Cr(VI) has excellent stability.

3.8. Comparison of adsorption capacity between adsorbents

The experimental results show that the pine nut shell and acid-modified bentonite have excellent adsorption capability to Cr(VI). For an easy comparison, the adsorption capacity of natural Akadama clay, tobacco residues, *Aegle marmelos* fruit shell, sugarcane bagasse, maize corn cob, jatropha oil cake, volcanic rocks, riverbed sand, Turkish montmorillonite clay, and orange peels powder were investigated. As shown in Table 5, the adsorption capability of pine nut shell and acid-modified bentonite to Cr(VI) is higher than that of the other adsorbents. It is reasonable to believe that pine nut shell and acid-modified bentonite can be used as a high-efficiency adsorbent for the treatment of Cr(VI) containing wastewater.

4. Conclusions

Using a large number of batch tests, the adsorption characteristics of Cr(VI) onto fly ash, pine nut shells, and acid-modified bentonite were investigated, and the influence of the solid-to-liquid ratio, pH, reaction time, initial concentration, temperature, and ionic strength on Cr(VI) adsorption characteristics was analyzed. The isothermal adsorption model, the kinetic adsorption model, and the adsorption

thermodynamic model were used to fit the test data, and the conclusions are listed below.

- The removal rates of Cr(VI) by the three adsorbents increase with increasing solid-to-liquid ratio, while the unit adsorption capacity decreases.
- Acidic environment promotes the adsorption of Cr(VI) onto the three adsorbents. The capacity of adsorbents to adsorb Cr(VI) is maximized when the pH of the solution is 1–3.
- Cl^- in the solution can affect the capability of adsorbents to adsorb Cr(VI). The adsorption capability of three adsorbents all reduced with increasing Cl^- concentration.
- The adsorption processes of three adsorbents all constitute rapid reactions, of which the adsorption reaction of acid-modified bentonite is the fastest. All adsorption processes reach equilibrium within 180 min. The pseudo-second-order kinetic model can accurately simulate the kinetic processes of Cr(VI) adsorption onto adsorbents.
- The adsorption of Cr(VI) onto fly ash is a spontaneous exothermic reaction, whereas the adsorption processes onto pine nut shells and acid-modified bentonite are nonspontaneous endothermic reactions. The isothermal adsorption process onto the fly ash can be described by Langmuir model, Freundlich model, and Redlich–Peterson model. However, the isothermal adsorption process onto pine nut shells can be described by Langmuir model and Redlich–Peterson model, and acid-modified bentonite can be described by Langmuir model, Temkin model, and Redlich–Peterson model.
- Desorption test results showed that all three adsorbents exhibit excellent stability, and pine nut shell, and acid-modified bentonite are more suitable for the treatment of Cr(VI) containing wastewater.

Acknowledgments

This study was supported by the Special Fund for Scientific Research by Shaanxi Provincial Education

Department (18JK1199) and Special Fund for Scientific Research by Xijing University (XJ18T01).

Symbols

b	—	Langmuir model constant, L/mg
b_T	—	Temkin constant, kJ/mol
C_0	—	Initial concentrations of heavy metal ions, mg/L
C_e	—	Equilibrium concentrations of heavy metal ions, mg/L
h	—	Initial adsorption rate, g/mg/min
k_1	—	Adsorption rate constant, 1/min
k_2	—	Adsorption rate constant, g/mg/min
K_D	—	Distribution coefficient at the solid-liquid interface, mL/g
K_F	—	Model constant related to the adsorption capacity, mg/g
K_T	—	Equilibrium binding constant, L/g
m	—	Mass of the clay or bentonite, g
n	—	Model constant related to adsorption strength
q_e	—	Adsorption capacity at equilibrium, mg/g
Q	—	Single-layer maximum adsorption capacity, mg/g
q_t	—	Adsorption capacities at time t , mg/g
R_L	—	Dimensionless separation factor
R	—	Removal rate, %
r	—	Solid-to-liquid ratio, g/L
T	—	Thermodynamic temperature, K
V	—	Volume of the solution, L
α	—	Isotherm constants, L/mg
β	—	Isotherm constants
ΔG	—	Gibbs free energy, kJ/mol
ΔH	—	Enthalpy change, kJ/mol
ΔS	—	Entropy change, J/mol/K

References

- [1] K.Y. Tang, Sources and harmfulness of chromium pollution, *J. Leather Sci. Eng.*, 7 (1997) 33–38.
- [2] J.O. Esalah, M.E. Weber, J.H. Vera, Removal of lead from aqueous solutions by precipitation with sodium diphosphonate, *Sep. Purif. Technol.*, 18 (1999) 25–36.
- [3] M. Lei, M. Tanaka, B.H. Liao, B.Q. Tie, P.F. Qin, Treatment of heavy metals from wastewater containing EDTA with sulfide precipitation, *Res. Environ. Sci.*, 21 (2008) 150–154.
- [4] S. Ahmed, S. Chughtai, M.A. Keane, The removal of cadmium and lead from aqueous solution by ion exchange with Na Y zeolite, *Sep. Purif. Technol.*, 13 (1998) 57–64.
- [5] M.M. Shi, M.Y. Liu, Y.L. Zeng, S.P. Su, Y.X. Cheng, Study on adsorption of Zn^{2+} , Pb^{2+} and Cd^{2+} on diatomite and bentonite, *Environ. Chem.*, 31 (2012) 162–167.
- [6] R.S. Juang, R.C. Shiau, Metal removal from aqueous solutions using chitosan-enhanced membrane filtration, *J. Membr. Sci.*, 165 (2000) 159–167.
- [7] N. Zheng, X.Y. Hua, D.M. Dong, L. Ji, Competitive adsorption of metal cations onto natural surface coatings, *J. Jilin Univ.*, 43 (2005) 388–393.
- [8] V.K. Gupta, A.K. Shrivastava, N. Jain, Biosorption of chromium(VI) from aqueous solutions by green algae *spirogyra* species, *Water Res.*, 35 (2001) 4079–4085.
- [9] X.Q. Xu, X.M. Li, Q. Yang, G.M. Zeng, K. Jin, Immobilized microorganism technology and its application in heavy metal wastewater treatment, *Technol. Equip. Environ. Pollut. Control*, 7 (2006) 99–105.
- [10] E. Pehlivan, T. Altun, S. Cetin, M.I. Bhangar, Lead sorption by waste biomass of hazelnut and almond shell, *J. Hazard. Mater.*, 167 (2009) 1203–1208.
- [11] Z. Zhao, Z.J. Xu, X.Y. Qiu, T.X. Liu, Preparation of anion-cationic organic bentonite and its adsorption of lead ions, *Chin. J. Environ. Eng.*, 6 (2012) 4405–4411.
- [12] B. Sandrine, N. Ange, B.A. Didier, C. Eric, S. Patrick, Removal of aqueous lead ions by hydroxyapatites: equilibria and kinetic processes, *J. Hazard. Mater.*, 139 (2007) 443–446.
- [13] Z.X. Chen, X.Y. Jin, J. Su, Z.L. Chen, Adsorption of cadmium(II) ions in aqueous solution using 1, 10-phenanthroline-modified immobilized bentonite, *Guangzhou Chem.*, 36 (2011) 5–10.
- [14] S.P. Deng, Adsorption treatment of cadmium-containing wastewater using modified rectorite, *Environ. Prot. Chem. Ind.*, 29 (2009) 308–311.
- [15] Y.H. Xi, H. Zhao, Z.X. Hu, Study on the adsorption of Ni^{2+} by fly ash, clay, silty clay and bentonite, *Chin. J. Geotech. Eng.*, 27 (2005) 59–63.
- [16] G. Sharma, M. Naushad, D. Pathania, A. Kumar, Multifunctional nanocomposite pectin thorium(IV) tungstomolybdate for heavy metal separation and photoremediation of malachite green, *Desal. Water Treat.*, 57 (2016) 19443–19455.
- [17] G. Sharma, B. Thakur, M. Naushad, A.H. Al-Muhtaseb, A. Kumar, M. Sillanpaa, G.T. Mola, Fabrication and characterization of sodium dodecyl sulphate@ironsilicophosphate nanocomposite: ion exchange properties and selectivity for binary metal ion, *Mater. Chem. Phys.*, 193 (2017) 129–139.
- [18] G. Sharma, B. Thakur, M. Naushad, A. Kumar, F.J. Stadler, S.M. Alfadul, G.T. Mola, Applications of nanocomposite hydrogels for biomedical engineering and environmental protection, *Environ. Chem. Lett.*, 16 (2018) 113–146.
- [19] G. Sharma, D. Pathania, M. Naushad, Preparation, characterization and antimicrobial activity of biopolymer based nanocomposite ion exchanger pectin zirconium(IV) selenotungstophosphate: application for removal of toxic metals, *J. Ind. Eng. Chem.*, 20 (2014) 4482–4490.
- [20] G. Sharma, M. Naushad, A. Kumar, S. Rana, S. Sharma, A. Bhatnagar, F.J. Stadler, A.A. Ghfar, M.R. Khan, Efficient removal of coomassie brilliant blue R-250 dye using starch/poly (alginate acid-cl-acrylamide) nanohydrogel, *Process Saf. Environ. Prot.*, 109 (2017) 301–310.
- [21] M. Naushad, T. Ahamad, G. Sharma, A.H. Al-Muhtaseb, A.B. Albadarin, M.M. Alam, Z.A. Allothman, S.M. Alshehri, A.A. Ghfar, Synthesis and characterization of a new starch/SnO₂ nanocomposite for efficient adsorption of toxic Hg^{2+} metal ion, *Chem. Eng. J.*, 300 (2016) 306–316.
- [22] M. Naushad, Surfactant assisted nano-composite cation exchanger: development, characterization and applications for the removal of toxic Pb^{2+} from aqueous medium, *Chem. Eng. J.*, 235 (2014) 100–108.
- [23] M. Naushad, G. Sharma, A. Kumar, S. Sharma, A.A. Ghfar, A. Bhatnagar, F.J. Stadler, M.R. Khan, Efficient removal of toxic phosphate anions from aqueous environment using pectin based quaternary amino anion exchanger, *Int. J. Biol. Macromol.*, 106 (2018) 1–10.
- [24] D. Pathania, G. Sharma, M. Naushad, V. Priya, A biopolymer-based hybrid cation exchanger pectin cerium(IV) iodate: synthesis, characterization, and analytical applications, *Desal. Water Treat.*, 57 (2015) 468–475.
- [25] Z.A. Al-Othman, R. Ali, M. Naushad, Hexavalent chromium removal from aqueous medium by activated carbon prepared from peanut shell: adsorption kinetics, equilibrium and thermodynamic studies, *Chem. Eng. J.*, 184 (2012) 238–247.
- [26] A. Kumar, A. Kumar, G. Sharma, M. Naushad, R.C. Veses, A.A. Ghfar, F.J. Stadler, M.R. Khan, Solar-driven photodegradation of 17- β -estradiol and ciprofloxacin from waste water and CO₂ conversion using sustainable coal-char/polymeric-g-C₃N₄/RG0 metal-free nano-hybrids, *New J. Chem.*, 18 (2017) 1–37.
- [27] L.X. Huang, C.Q. Cao, D.Y. Xu, Q.J. Guo, F. Tan, Intrinsic adsorption properties of raw coal fly ash for quinoline from aqueous solution: kinetic and equilibrium studies, *SN Appl. Sci.*, 1 (2019) 1–8.
- [28] H.X. Zhou, R. Bhattarai, Y.K. Li, S.Y. Li, Y.H. Fan, Utilization of coal fly and bottom ash pellet for phosphorus adsorption: sustainable management and evaluation, *Resour. Conserv. Recycl.*, 149 (2019) 372–380.

- [29] C.W. Ye, B.W. Yan, X. Ji, B. Liao, R. Gong, X.J. Pei, G. Liu, Adsorption of fluoride from aqueous solution by fly ash cenospheres modified with paper mill lime mud: experimental and modeling, *Ecotoxicol. Environ. Saf.*, 180 (2019) 366–373.
- [30] M.E. Alouani, S. Alehyen, M.E. Achouri, M. Taibi, Comparative study of the adsorption of micropollutant contained in aqueous phase using coal fly ash and activated coal fly ash: kinetic and isotherm studies, *Chem. Data Collect.*, 23 (2019) 100265.
- [31] M. Naushad, M.A. Khan, Z.A. Allothman, M.R. Khan, M. Kumar, Adsorption of methylene blue on chemically modified pine nut shells in single and binary systems: isotherms, kinetics, and thermodynamic studies, *Desal. Water Treat.*, 57 (2016) 15848–15861.
- [32] U.A. Qureshi, A.R. Solangi, S.Q. Memon, S.I.H. Taqvi, Utilization of pine nut shell derived carbon as an efficient alternate for the sequestration of phthalates from aqueous system, *Arabian J. Chem.*, 7 (2014) 1166–1177.
- [33] A. Esmaili, H. Eslami, Efficient removal of Pb(II) and Zn(II) ions from aqueous solutions by adsorption onto a native natural bentonite, *MethodsX*, 6 (2019) 1979–1985.
- [34] T. Şahan, Application of RSM for Pb(II) and Cu(II) adsorption by bentonite enriched with-SH groups and a binary system study, *J. Water Process Eng.*, 31 (2019) 100867.
- [35] H.M. Cheng, Q. Zhu, Z.P. Xing, Adsorption of ammonia nitrogen in low temperature domestic wastewater by modification bentonite, *J. Cleaner Prod.*, 233 (2019) 720–730.
- [36] B. Sadeghalvad, A.R. Azadmehr, H. Motevalian, Statistical design and kinetic and thermodynamic studies of Ni(II) adsorption on bentonite, *J. Cent. South Univ.*, 24 (2017) 1529–1536.
- [37] P.R. Souza, G.L. Dotto, N.P.G. Salau, Analysis of intraparticle diffusion on adsorption of crystal violet on bentonite, *Chem. Eng. Commun.*, 206 (2019) 1474–1484.
- [38] L. Mdlalose, M. Balogun, K. Setshedi, L. Chimuka, A. Chetty, Adsorption of phosphates using transition metals-modified bentonite clay, *Sep. Sci. Technol.*, 54 (2019) 2397–2408.
- [39] D.D. Do, *Adsorption Analysis: Equilibria and Kinetics*, Imperial College Press, London, 1998.
- [40] S.S. Majumdar, S.K. Das, R. Chakravarty, T. Saha, T.S. Bandyopadhyay, A.K. Guha, A study on lead adsorption by *Mucor rouxii* biomass, *Desalination*, 251 (2010) 96–102.
- [41] B.H. Hameed, J.M. Salman, A.L. Ahmad, Adsorption isotherm and kinetic modeling of 2,4-D pesticide on activated carbon derived from date stones, *J. Hazard. Mater.*, 163 (2009) 121–126.
- [42] S.K. Behera, J.H. Kim, X.J. Guo, H.S. Park, Adsorption equilibrium and kinetics of polyvinyl alcohol from aqueous solution on powdered activated carbon, *J. Hazard. Mater.*, 153 (2008) 1207–1214.
- [43] M.I. Temkin, V. Pyzhev, Kinetics of ammonia synthesis on promoted iron catalysts, *Acta Physicochim. URSS*, 12 (1940) 327–356.
- [44] O. Redlich, D.L. Peterson, A useful adsorption isotherm, *J. Phys. Chem.*, 63 (1959) 1024–1026.
- [45] S. Langergren, About the theory of so-called adsorption of soluble substances, *Kungl. Svenska Vetenskapskad. Handl.*, 24 (1898) 1–39.
- [46] Y.S. Ho, G. McKay, Pseudo-second order model for sorption processes, *Process Biochem.*, 34 (1999) 451–465.
- [47] L.Z. Song, C.Y. Dong, Z.J. Zhang, Q.Y. Zheng, Adsorption behavior of Cu(II) ion by the polyacrylic acid-polyvinylidene fluoride blending resin, *China Environ. Sci.*, 28 (2007) 322–326.
- [48] H.S. Jia, H.H. Liu, C.W. Yu, S. Hu, J. Zhou, Molybdenum-containing wastewater treatment effect of fly ash and its adsorption mechanism, *Rare Met. Cem. Carbides*, 40 (2012) 73–76.
- [49] S.X. Ren, The speciation of chromium in water, *China Environ. Sci.*, 9 (1989) 40–44.
- [50] S.B. Wang, Y. Boyjoo, A. Choueib, Z.H. Zhu, Removal of dyes from aqueous solution using fly ash and red mud, *Water Res.*, 39 (2005) 129–138.
- [51] L.J. Han, Research on Adsorption Behavior of DNBP on Fly Ash and Modified Fly Ash, Master Dissertation of Dalian University of Technology, Dalian, 2007.
- [52] G.D. Yang, Study on the Adsorption of Chromium(VI) in Wastewater by Peanut Shell, Master Dissertation of Lanzhou University of Technology, Lanzhou, 2009.
- [53] R.X. Li, D.F. Xu, C.P. Yang, L.P. Wang, Study on adsorption and mechanism of anionic surfactant in wastewater by fly ash, *Ind. Saf. Environ. Prot.*, 38 (2012) 6–8.
- [54] W.H. Zou, R.P. Han, Z.Z. Chen, J.H. Zhang, J. Shi, Kinetic study of adsorption of Cu(II) and Pb(II) from aqueous solutions using manganese oxide coated zeolite in batch mode, *Colloids Surf., A*, 279 (2006) 238–246.
- [55] Y. Zhao, S. Yang, D. Ding, J. Chen, Y. Yang, Z. Lei, C. Feng, Z. Zhang, Effective adsorption of Cr(VI) from aqueous solution using natural Akadama clay, *J. Colloid Interface Sci.*, 395 (2013) 198–204.
- [56] M. Kilic, E. Apaydin-Varol, A.E. Pütün, Adsorptive removal of phenol from aqueous solutions on activated carbon prepared from tobacco residues: equilibrium, kinetics and thermodynamics, *J. Hazard. Mater.*, 189 (2011) 397–403.
- [57] R. Gottipati, S. Mishra, Preparation of microporous activated carbon from *Aegle marmelos* fruit shell and its application in removal of chromium(VI) from aqueous phase, *J. Ind. Eng. Chem.*, 36 (2016) 355–363.
- [58] U.K. Garg, M.P. Kaur, V.K. Garg, D. Sud, Removal of hexavalent chromium from aqueous solution by agricultural waste biomass, *J. Hazard. Mater.*, 140 (2007) 60–68.
- [59] E. Alemayehu, S. Thiele-Bruhn, B. Lennartz, Adsorption behaviour of Cr(VI) onto macro and micro-vesicular volcanic rocks from water, *Sep. Purif. Technol.*, 78 (2011) 55–61.
- [60] Y.C. Sharma, C.H. Weng, Removal of chromium(VI) from water and wastewater by using riverbed sand: kinetic and equilibrium studies, *J. Hazard. Mater.*, 142 (2007) 449–454.
- [61] S.T. Akar, Y. Yetimoglu, T. Gedikbey, Removal of chromium(VI) ions from aqueous solutions by using Turkish montmorillonite clay: effect of activation and modification, *Desalination*, 244 (2009) 97–108.
- [62] K. Malook, Ihsan-ul-Haque, Investigation of aqueous Cr(VI) adsorption characteristics of orange peels powder, *Prot. Met. Phys. Chem.*, 55 (2019) 34–40.